Motor Sequences - Separating The Sequence From The Motor.

A longitudinal rsfMRI Study

ATP Jäger[1,], JM Huntenburg[2], SA Tremblay[3,4], U Schneider[1,], S Grahl[5] , J Huck[3], CL Tardif[6,7], A Villringer[1,8,9,10], CJ Gauthier[3,4], PL Bazin[1,11]*, CJ Steele[1,12]*

[1] Department of Neurology, Max Planck Institute for Human Cognitive and Brain Sciences, Leipzig, Germany
[2] Neuroscience Programme, Champalimaud Research, Lisbon, Portugal
[3] Department of Physics/PERFORM center, Concordia University, Montreal, QC, Canada
[4] Montreal Heart Institute, Montreal, QC, Canada
[5] Clinic of Neurology, Technical University Munich, Germany
[6] Department of Biomedical Engineering, McGill University, Montreal, QC, Canada
[7] Montreal Neurological Institute, Montreal, QC, Canada
[8] Clinic for Cognitive Neurology, Leipzig, Germany
[9] Leipzig University Medical Centre, IFB Adiposity Diseases, Leipzig, Germany
[10] Collaborative Research Centre 1052-A5, University of Leipzig, Germany
[11] Faculty of Social and Behavioral Sciences, University of Amsterdam, Netherlands
[12] Department of Psychology, Concordia University, Montreal, QC, Canada

* These two authors contributed equally to this work.

Abstract

In motor learning, sequence-specificity, i.e. the learning of specific sequential associations, has predominantly been studied using task-based fMRI paradigms. However, offline changes in resting state functional connectivity after sequence-specific motor learning are less well understood. Previous research has established that plastic changes following motor learning can be divided into stages including fast learning, slow learning and retention. A description of how resting state functional connectivity after sequence-specific motor sequence learning (MSL) develops across these stages is missing. This study aimed to identify plastic alterations in whole-brain functional connectivity after learning a complex motor sequence by contrasting an active group who learned a complex sequence with a control group who performed a control task matched for motor execution. Resting state fMRI and behavioural

performance were collected in both groups over the course of 5 consecutive training days and at follow-up after 12 days to encompass fast learning, slow learning, overall learning and retention. Between-group interaction analyses showed sequence-specific increases in functional connectivity during fast learning in the sensorimotor territory of the internal segment of right globus pallidus (GPi), and sequence-specific decreases in right supplementary motor area (SMA) in overall learning. We found that connectivity changes in key regions of the motor network including the superior parietal cortex (SPC) and primary motor cortex (M1) were not a result of sequence-specific learning but were instead linked to motor execution. Our study confirms the sequence-specific role of SMA and GPi that has previously been identified in online task-based learning studies in humans and primates, and extends it to resting state network changes after sequence-specific MSL. Finally, our results shed light on a timing-specific plasticity mechanism between GPi and SMA following MSL.

Keywords: Motor Sequence Learning, rsfMRI, sequence-specificity

Introduction:

Motor learning induced brain plasticity has been typically studied using magnetic resonance imaging (MRI) (for review, see Dayan & Cohen, 2011; Krakauer et al, 2019; Taubert et al., 2012), from immediate online functional changes (Coynel et al., 2010, Karim et al., 2017, Steele & Penhune, 2010; Yokoi & Diedrichsen, 2019) to long term structural effects (Gryga et al., 2012, Taubert et al., 2010, Bengtsson et al., 2005; Scholz et al., 2009). While task-based studies investigate immediate training-related processes during task performance and structural studies usually identify longer term changes in brain morphometry they cannot comment on how the learned skill is represented and maintained within functional networks

of the brain outside of the training/learning context. Resting state fMRI (rsfMRI) can be used to investigate functional plasticity that occurs between online functional and slower structural changes. Measured in the absence of a task, resting-state network dynamics are thought to reflect the previous co-activation of functionally connected brain regions (Biswal et al., 1994, Guerra-Carrillo et al., 2014). Alterations in these functional networks are thought to reflect the strengthening of the memory trace generated during practice (Albert et al, 2009, Lewis et al., 2009, Vahdat et al., 2011). Therefore, assessing resting state networks and how they change in response to training can provide unique insight into training-related functional plasticity beyond the immediate time point of learning.

Previous research in motor learning has established that sequence learning *per se* can be distinguished from motor execution (Rosenbaum et al., 1983, Penhune and Steele, 2012, Wiestler & Diedrichsen, 2013). However, while this concept has been assessed, tested and discussed in task-based studies (Seidler et al., 2002; Yokoi and Diedrichsen, 2019, Wymbs & Grafton, 2015), learning that is specific to sequential associations (i.e., sequence-specific learning) is rarely if ever differentiated from motor execution in rsfMRI studies of motor learning. In part, this is due to the added challenge of including additional control groups matched for motor execution. Conclusions about functional changes being the result of sequence-specific learning, and not simply an effect of repeated performance, cannot be made without the inclusion of a control group (Thomas and Baker, 2013, Steel et al. 2019). As a result, it is currently unclear which regions of the sensorimotor network are involved in offline sequence-specific learning versus those more generally involved in motor execution.

RsfMRI connectivity changes after motor sequence learning (MSL) have been investigated with “pre/post” frameworks where resting state functional connectivity (rsFC) is typically measured only before and/or after performing the task to identify immediate and overnight

effects (Sami and Miall, 2013, Gregory et al., 2014, Sami et al., 2014, Mary et al., 2017, Albert et al., 2009). And while motor learning is thought to progress through several stages involving rapid changes in performance (fast learning), slower improvements over a longer time period (slow learning), and maintenance of robust performance (retention) (Doyon & Benali, 2005, Dayan and Cohen, 2011, Lohse et al., 2014), there are few studies that have followed changes in rsfMRI networks after MSL across multiple sessions of training to investigate larger timescales (Ma et al., 2011, Xiong et al., 2009). To our knowledge, there has been no investigation of sequence-specific resting state network plasticity across all three stages of learning. The present study is the first to address this gap.

Here, participants learned a continuous motor task with their right (dominant) hand over five days of training, followed by a retention probe 12 days later. RsfMRI was collected five times over the course of the training, providing a rich sampling of the different stages of learning in the absence of performance. Crucially, participants were randomly assigned to either a training (sequence-specific training) or control group (matched for motor execution). This rich dataset allowed us to identify the brain regions involved in sequence-specific learning and explore their functional dynamics.

Methods:

Participants:

40 right-handed healthy participants with no history of neurological disorder (22 females, ranging from 20 to 32 years of age, M ± SD: 24.5 ± 2.44) were included in this study. Participants were recruited from the database of the Max Planck Institute for Human Cognitive and Brain Sciences in Leipzig, Germany and randomly assigned to an experimental (N=20, 11 females) and control group (N=20, 10 females). The experimental group learned a

previously published complex visuomotor sequence pinch-force task (Gryga et al., 2012) while the control group performed a much simpler sinusoidal sequence that required almost no learning to perform. The training period consisted of 5 days, with an additional familiarization session prior to training and a retention session following 12 days without practice. Participants did not meet any MRI exclusion criteria, gave written informed consent in accordance with the Declaration of Helsinki, and were monetarily compensated for their time. The study design was approved by the ethics review board of the Medical Faculty of the University of Leipzig.

Task and Stimuli: Sequential Pinch Force Task

The Sequential Pinch Force Task (SPFT) is a motor sequence task that requires the participant to use the index finger and thumb of the dominant (right) hand to exert force on the end of a pinch force device (Fig. 1a) which measures force at a sample rate of 80Hz. This pinching force controls the height of a rectangular yellow force bar (FOR) that is displayed on the screen (Fig. 1b).

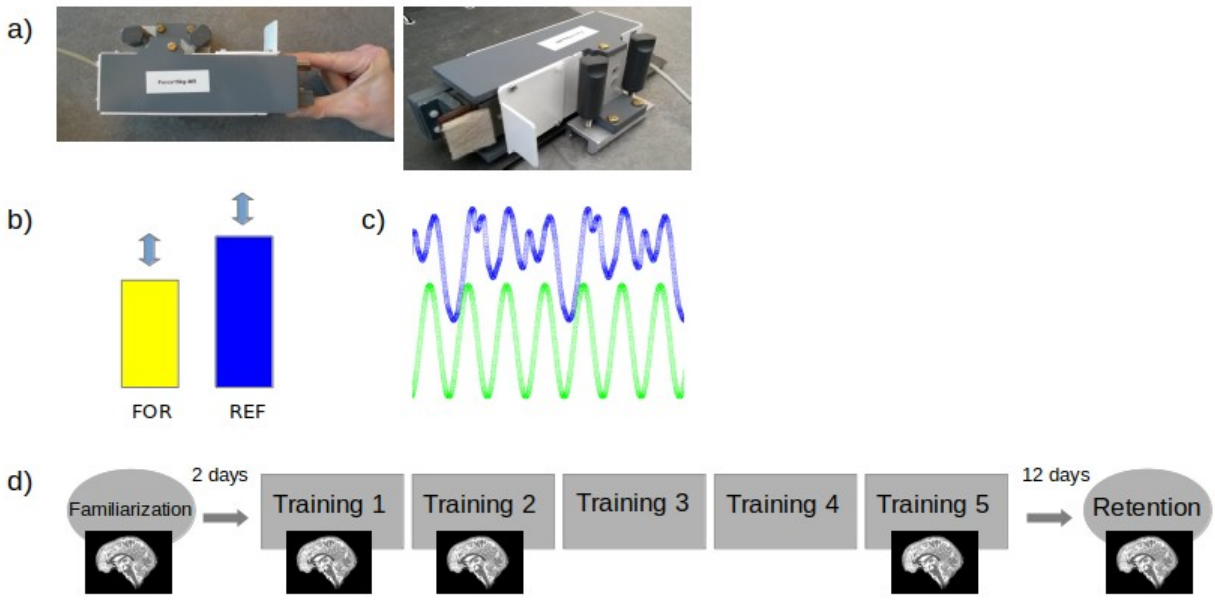

Fig. 1. **Task and Procedure** - a) Sequential Pinch Force Task (SPFT) device, b) Visual screen representations: FOR bar (yellow) REF bar (blue), c) Pinch-force task, green: simple control condition (SMP) sequence, blue: learning condition (LRN) sequence d) experimental design. Brain images indicate sessions where 7T scanning was performed.

In the SPFT, the participant is instructed to adjust the height of FOR to match that of an adjacent blue reference (REF) bar. The up and down movement of REF follows a pre-set sequence (Figure 1b, 1c). There are 3 conditions: a learning condition (LRN), a simple control condition (SMP) and a resting condition (RST). In LRN, the movement of the bar follows a previously published sequence of varying heights that is difficult to predict (Fig. 1c) and learned over time (Gryga, 2012), while the SMP sequence is a simple sinusoid. The SMP sequence was designed to match the LRN sequence for its frequency of maximum power, duration, range, and the total magnitude of force. While in the SMP condition participants merely performed this predictable and unvarying sinusoidal sequence of motor movements; in the LRN condition participants execute the same *type* of movements (i.e., varying pinch force over time) but performed a more complex sequence (Figure 1c). As a

result, SMP serves as a matched control for motor execution which, in comparison with LRN, can be used to identify sequence-specific differences that are over and above any changes associated with motor execution. During RST, both bars are displayed statically at 50% of their maximum height and participants were instructed to focus their gaze between the upper edges of the two bars.

On each training day, 3 blocks consisting of 3 SMP, LRN and RST trials each were performed by the experimental group; for a total of 9 trials per condition on each day. The control group performed the same number of blocks and trials but never performed LRN: the LRN blocks were replaced by SMP blocks such that the total effort for each group remained the same. Each trial was 18 seconds in length. After the SMP and LRN trials, participants received feedback consisting of their average accuracy in matching the heights of REF and FOR.

For simplicity, we will refer to the groups based on which sequence they were assigned throughout the rest of this paper: SMP (SMP only) vs. LRN (SMP and LRN).

Training and Experimental Procedure:

The experimental procedure (Fig. 1d) consisted of one familiarization session (d0), five training sessions (d1-d5) and one retention session (d17, which took place 12 days after d5). The first training session (d1) always took place on Monday and the d0 familiarization session took place on the previous Friday so that the training period for each participant always took place on five consecutive days (Monday-Friday). The familiarization session included a maximum force calibration step followed by 9 trials of the SMP sequence. When measuring the maximum pinch force, the subject was asked to pinch the device with as much force as possible for ten seconds and the maximum value obtained during this period was considered maximum force. This measurement was used to calibrate the level of force

required to move the visually presented force bar and was set to between 5% (minimum bar level) and 30% (maximum bar level) of each individual's maximum force to ensure that participants were also matched by relative effort. Five sessions (d0, d1, d2, d5, d17) were performed while lying supine inside of the MRI scanner and two (d3, d4) outside of the scanner in a separate testing room while seated at a computer. During these sessions, the SPFT was performed with the dominant hand, over a total duration of 20 minutes (3 blocks, 9 trials [LRN group: 3x(LRN), 3x(SMP), 3x(RST); SMP group: 3x(SMP), 3x(SMP), 3x (RST)]). The d17 retention session followed the same protocol as the training days and was measured 12 days after the last day of the training period. All sessions took place at the same time during the day to account for potential time of day fluctuations in resting state connectivity (Steel et al. 2019).

MRI protocol:

MRI data were acquired on a 7 Tesla MRI scanner (MAGNETOM, Siemens Healthcare, Erlangen, Germany) equipped with a 32-channel head coil (Nova). For the purposes of the current study, blood-oxygenation-level dependent (BOLD) rsfMRI, MP2RAGE T1 (Marques et al., 2010), and a fieldmap were acquired. RsfMRI scans [BOLD, voxel dimensions = 1.2 x 1.2 x 1.2mm, 512 whole brain volumes, FOV = 192 x 192 mm², slice acceleration factor: 2, slice thickness = 1mm, 102 slices, GRAPPA factor 2, partial Fourier 6/8, TR = 1130ms, TE = 22ms, flip angle = 40°, bandwidth = 1562 Hz/Px] were acquired under an eyes open condition with a fixation cross for 10 minutes and took place before the task. Additionally, MP2RAGE images [voxel dimensions = 0.7 x 0.7 x 0.7mm, FOV = 224 x 224 x 240mm³, TR = 5000ms, TE = 2.45ms, flip angle 1 = 5°, flip angle 2 = 3°, bandwidth = 250 Hz/Px] and a fieldmap [voxel dimensions = 2 x 2 x 2mm, FOV = 256 x 256mm², slice thickness = 2mm, 80 slices, TR = 18ms, TE1 = 4.08ms, TE2 = 9.18ms, flip angle = 10°, bandwidth = 300 Hz/Px] were

also collected.

Image Processing

A custom preprocessing pipeline was implemented using Nipype (Gorgolewski et. al. 2011) and Nilearn (v0.2.3, Abraham et al., 2014). The first five volumes of the rsfMRI EPI sequences were removed for signal stabilization. Motion correction was performed using the SpaceTimeRealign algorithm (Roche, 2011) implemented in Nipy. Given the short TR, no slice timing correction was applied. Magnetic field inhomogeneity and subsequent image distortions are more pronounced at higher field strengths (Cusack et al., 2003), therefore EPI data were undistorted using the fieldmaps and FSL FUGUE (Jenkinson, 2004). Outliers in composite motion and average brain signal were detected using Nipype's ArtifactDetect function for removal in a subsequent step. Nilearn's high_variance_confounds function was used to extract time courses representative of physiological noise from the white matter and cerebrospinal fluid, following the aCompCor approach (Behzadi et al., 2007). Nuisance regression was performed using Nilearn's NiftiMasker and included the previously calculated 12 motion regressors (3 translations and 3 rotations plus their first derivatives), outlier regressors and physiological regressors. Timeseries were detrended, variance-normalized and bandpass filtered between 0.01-0.1 Hz. A 2.4 mm FWHM Gaussian spatial smoothing filter was applied to the preprocessed data (Poldrack et al., 2011). Degree centrality (DC) and Eigenvector centrality (EC) maps were calculated with the fast Eigenvector centrality mapping (fastECM) algorithm by Wink et al., (2012) in native space to protect data properties. Finally, a linear (12 degree of freedom (dof)) and nonlinear (Syn) registration to MNI space were performed with ANTS (Avants et al., 2009) as implemented in the CBS Tools (Bazin et al., 2014). Further preprocessing steps such as generating transformation maps between native, group and MNI spaces, as well as tissue segmentation of the

anatomical MP2RAGE images were performed using the CBS Tools. All scripts are openly available at https://github.com/AthSchmidt/MMPI/tree/master/preprocessing.

Network Analyses

In recent years, graph-based analyses have become increasingly used for studying functional connectivity (Sami and Miall, 2013, Wang, 2010 review). In such analyses, brain regions are treated as nodes – and several approaches have been used to describe the dynamics of connections between such nodes (Bullmore and Bassett, 2011). Graph based analyses also offer the possibility to undertake data-driven investigations of brain dynamics globally and quantifiably on a voxel level without prior assumptions. DC mapping is a simple way of describing network and node properties in which direct connections to other nodes are measured. Increases and decreases in DC are simply based on more or less connecting nodes, respectively. Comparing DC across different time points of learning offers rapid and direct insight into changes of network properties as a result of MSL. EC mapping is a more complex method to analyze network structures which identifies nodes that are of central importance to the entire network (Lohmann et al., 2010). The importance of nodes is determined by the connectedness to other nodes, increasing as the connection to nodes with many important connections also increases. In other words: nodes become more important to the network when they are connected to other important nodes, and are assigned higher EC values. Major advantages of DC and EC compared to other rsfMRI analysis methods are their faster computation times, and the fact that they are data driven and do not require additional assumptions (Wink et al, 2012). Since they have different sensitivities to local and global, as well as cortical and subcortical connectivities (Zuo et al., 2012), we used both DC and EC as complementary measures of centrality and therefore connectivity.

Applying both DC and EC, we analyzed node centrality on the whole brain level by treating

each voxel as a node. For analyses, voxel-wise DC or EC at each time point were compared between groups to infer connectivity changes as a result of sequence-specific motor learning. For example, the changes between d1 and d2 of the LRN group were compared to the changes between d1 and d2 of the SMP group in order to identify potential interaction effects. The comparisons between time points were interpreted as being reflective of the different learning stages. Based on the motor learning literature, we defined fast learning as changes between the first and second days of training (d1/d2), slow learning as improvements between the second and fifth days (d2/d5), overall learning from no knowledge of the task up until plateau (d1/d5) and retention as skill recall after the passage of time without training (d5/d17) (Dayan and Cohen, 2011).

Behavioral Analysis

We analyzed the behavioral data in order to characterize performance and contextualize our fMRI results within the different stages of sequence learning introduced by task-based fMRI studies. Performance was assessed by measuring temporal synchronization (SYN) which describes the deviation of FOR in milliseconds from REF (LRN or SMP). A cross-correlation between REF and FOR patterns was computed for each trial, and the time lag with the maximum correlation value was used to determine the degree of temporal synchronization (SYN), where a score of 0 denotes perfectly synchronized performance). Behavioural performance metrics were computed using custom-built MATLAB scripts (available at https://github.com/neuralabc/SPFT).

Statistical Analyses

In order to understand changes in performance as a result of training, we computed the mean SYN per day for each participant and performed a repeated measures ANOVA with factors day (1-17) and group (LRN vs. SMP). Mauchly’s tests were conducted to correct sphericity

when necessary (Greenhouse-Geisser if $\varepsilon < 0.75$ or Huynh Feldt if $\varepsilon > 0.75$). Post-hoc Tukey's tests were used to assess timing-specific significant effects between consecutive days. Statistical testing on the behavioral data was performed with the Jamovi software (https://www.jamovi.org; Singmann, 2018; Lenth, 2018) based on R (https://cran.r-project.org/).

Group X Time Interaction Analyses

For the rsFC whole brain interaction analyses we used a flexible factorial design for longitudinal data from the CAT12 Toolbox in SPM with two groups and 5 time points (d0, d1, d2, d5, d17). The flexible factorial design included two factors: group and time point. Within the interaction analyses, changes between time points within-group were compared across groups and learning stages. For example, when investigating the fast learning stage, the interaction analysis consisted of comparing both the d1-d2 contrast (decreases from d1 to d2, relative to LRN) and the d2-d1 contrast (increases from d1 to d2, relative to LRN). Interaction analyses were performed for the following time point contrasts: d1-d2, d2-d1, d2-d5, d5-d2, d1-d5, d5-d1, d5-d17, and d17-d5. Following the identification of interaction effects, we then computed the magnitude of change within the significant ROI in each group to determine which group was driving the effect. Based on our design, the identification of a change in centrality that was greater in the LRN group than the SMP group was considered as a sequence-specific effect. RsfMRI results are reported using cluster inference with the SPM default primary threshold of $p < 0.001$ and FDR correction at the cluster level at $p < 0.05$ (Woo et al., 2014).

Relationships between sequence-specific change in different regions

After acquiring information about local centrality changes in sequence-specific clusters, we were interested in how these clusters may be related on a network level. Under the hypothesis

that connectivity changes in sequence-specific clusters are dependent on one another, we conducted exploratory correlation analyses between centrality change scores across participants in all sequence-specific regions. As we found two sequence-specific clusters at two different time points, we first correlated their change values where they each showed significant change in the interaction analysis (GPi d1/d2 - SMA d1/d5). We then correlated change values at the same time points; comparing change values during fast learning (d1/d2) and overall learning (d1/d5). Therefore, we performed a total of three exploratory correlation analyses ([GPi d1/d2 - SMA d1/d5], [GPi d1/d2 - SMA d1/d2], [GPi d1/d5 - SMA d1/d5]) using the pearsonr function from the stats package within SciPy (Virtanen et al., 2020). The visualizations were created using seaborn's (Michael Waskom et al., 2020) regplot function in Python.

Results

Behavioral Results

Two outliers were excluded from the behavioral data because their values were more than 2 standard deviations away from the mean on two days. We found a significant main effect of group ($F(1,36) = 69.9$, $p < .001$, $\eta 2 = .66$) (Fig. 2). Post-hoc Tukey t-tests revealed significant differences in the LRN group between d1 and d2 ($t= 8.75$, $p <.001$), d2 and d3 ($t=4,69$, $p <.001$) and d3 and d4 ($t = 3.41$, $p =0.03$). There were no significant differences in the LRN group between days 4, 5 and 17. There were no significant differences between days in the SMP group, supporting the hypothesis that the SMP group was not learning. Therefore, we were able to see the progress of learning the LRN sequence over time (Fig. 2). There were no significant differences between the two groups in musical and physical exercise experience (all p-values > .05).

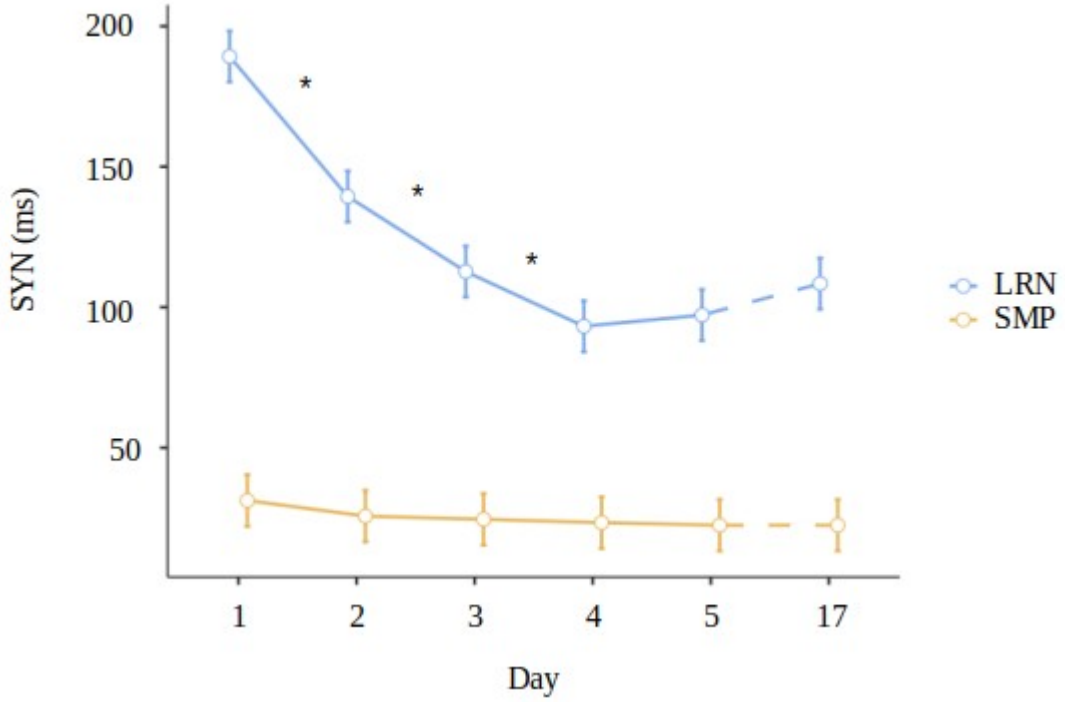

Fig. 2 Behavioral Results. Temporal synchronisation (SYN) for LRN and SMP across all days (d1-d17). Error bars indicate the standard error of the mean.

rsFC Results

Interaction effects - Fast Learning

When investigating changes in DC we found significant group by day interaction effects for the fast learning stage (contrasting d1 and d2) in the right posterior-ventro-medial part of the internal segment of globus pallidus (GPi), right superior occipital gyrus (SOG), right superior parietal cortex (SPC) and the hand region of the left primary motor cortex (M1) (Fig. 3a & b). Interaction effects were also found in EC during fast learning in the right anterior insular cortex (AIC) and the right SPC (Fig. 3c & d). However, further investigation (Table 3) revealed that only the cluster in the GPi was predominantly driven by changes in the LRN group and therefore considered sequence-specific change. Trajectories of change in DC and EC were plotted over all training days in significant clusters of the interaction analyses to provide additional context about the progression of changes within those regions across the

time points (Fig. 3b and 3e).

a)

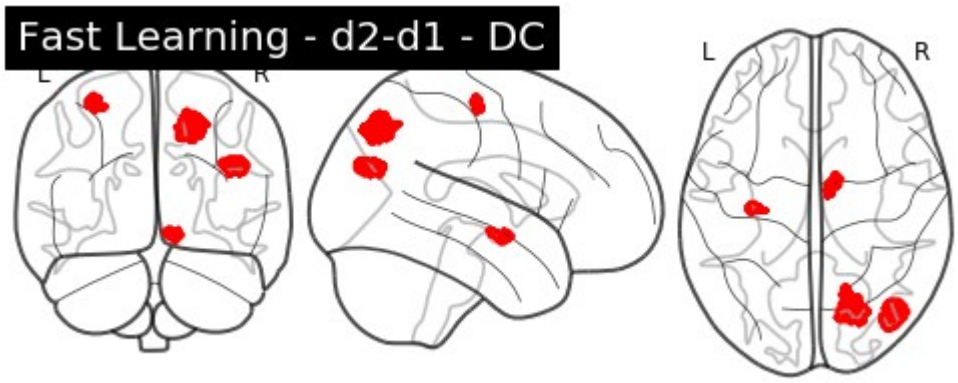

b)

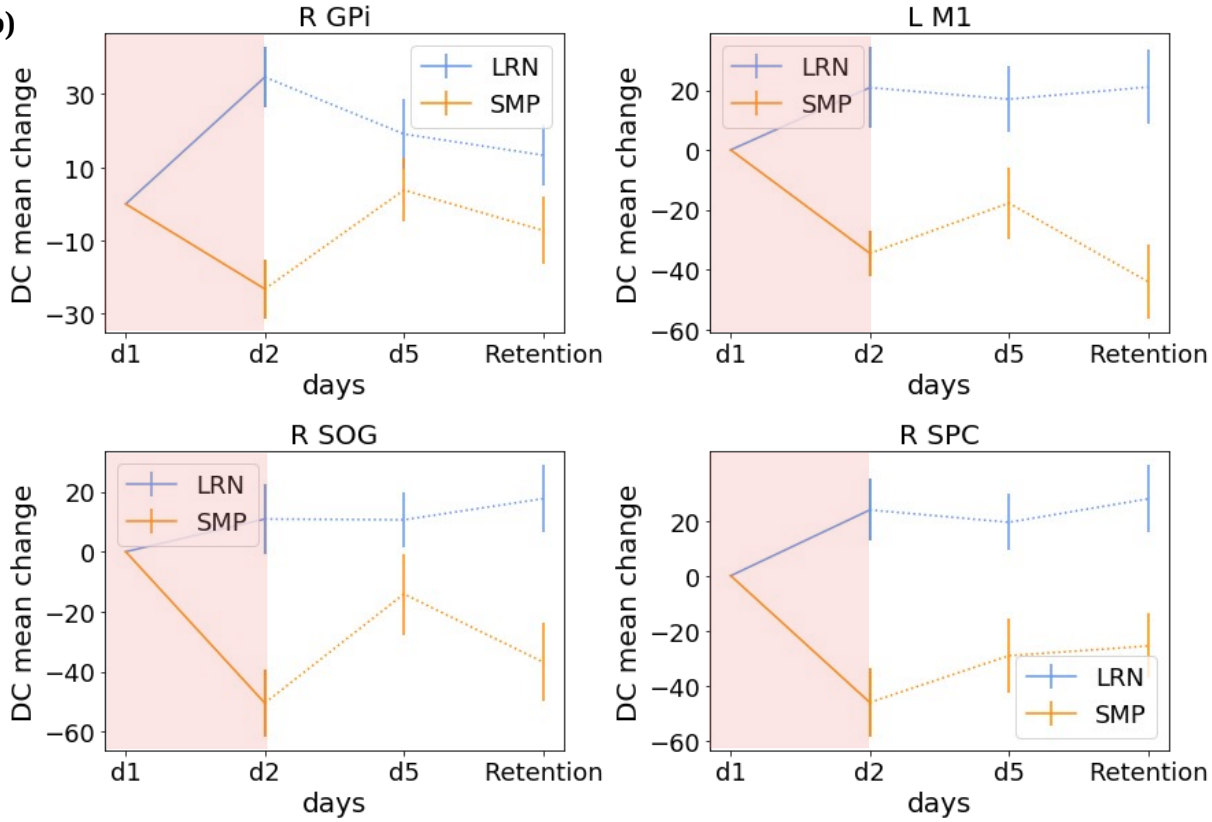

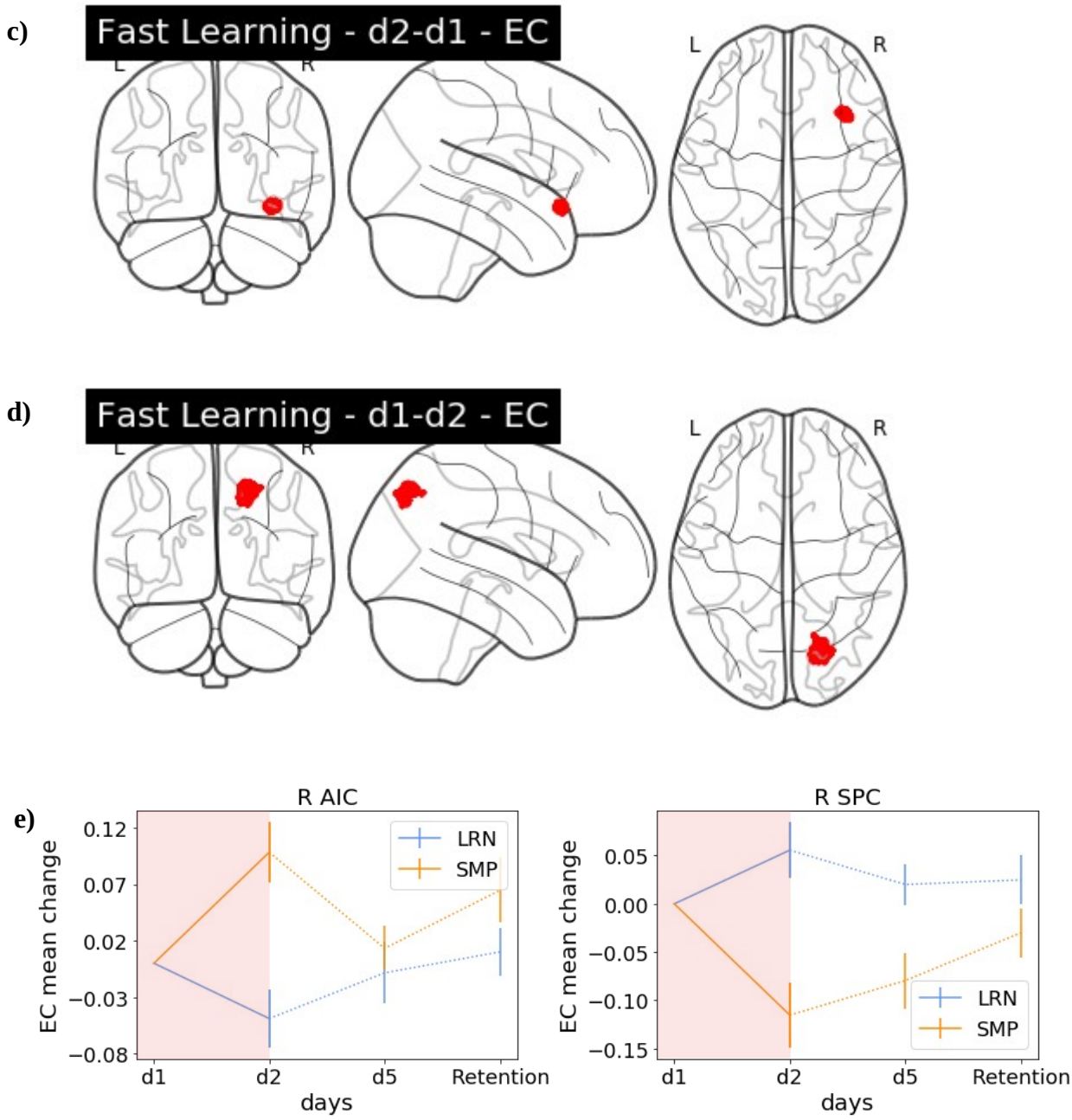

Figure 3: Group interaction: Fast learning. a) Glass brain DC. d2-d1 interaction effects in the hand region of left M1 as well as right SPC, right SOG and right GPi (seq-spec.) b) shows the DC change value trajectory over the entire training period for the significant clusters including R GPi, L M1, R SOG and R SPC displayed for LRN and SMP. The period which had the significant interaction (d1/d2) is highlighted in red. c) Glass brain EC. d1-d2 interaction effect in the right AIC d) Glass brain EC. d2-d1 interaction effect in the right SPC. e) shows the EC change value trajectory over the entire training period for the significant clusters including R AIC and R SPC displayed for LRN and SMP. The period which had the significant interaction (d1/d2) is highlighted in red.

Interaction effects - Slow Learning

Interaction effects between d2 and d5 were found in DC between groups in the right AIC (Fig. 4a). An overlapping cluster was significant for the same contrast in EC (Fig. 4b). However, neither of these clusters were sequence-specific, as the SMP group was driving the changes.

a)

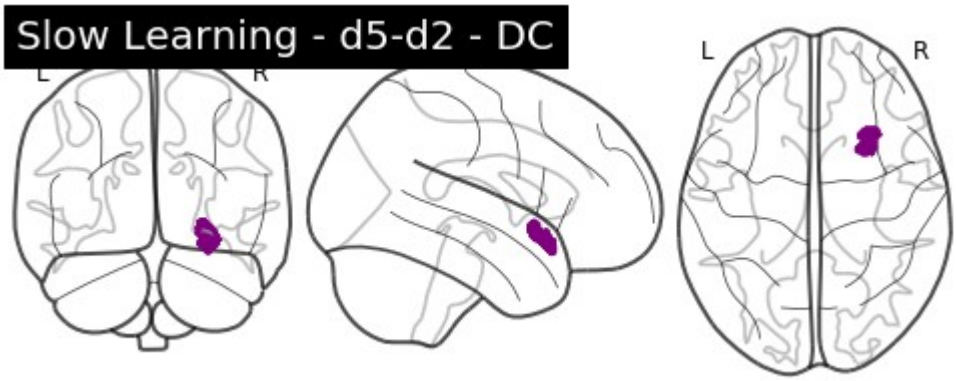

b)

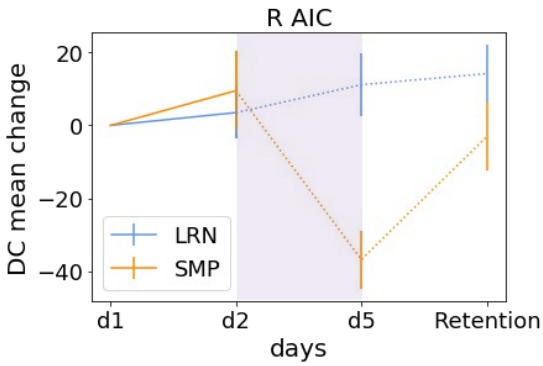

c)

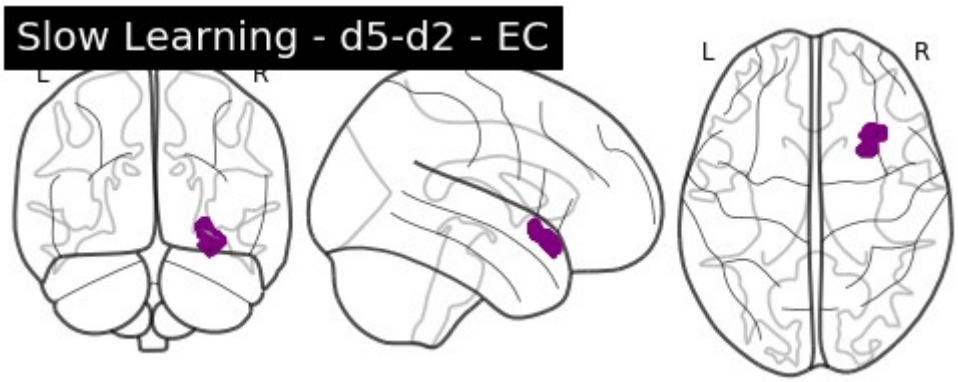

d)

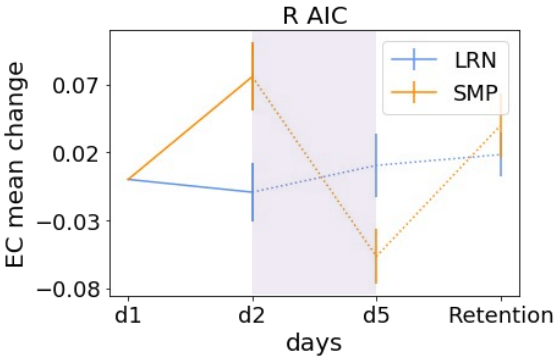

Fig. 4 Group interaction: Slow learning. a) Glass brain DC. d5-d2 interaction effects in the R AIC. b) shows the DC change value trajectory over the entire training period for the significant cluster in R AIC displayed for LRN and SMP with the period which had the significant interaction (d2/d5) highlighted in purple. c) Glass brain EC. d5-d2 interaction effects in the R AIC. d) shows the EC change value trajectory over the entire training period for the significant cluster in R AIC displayed for LRN and SMP with the period which had the significant interaction (d2/d5) highlighted in purple

Interaction effects - Overall Learning

We found interaction effects between groups on DC during overall learning (d1 vs d5) in the right Putamen and bilateral SPC (Fig. 5a).

We also compared d1 and d5 in EC between groups and found significant effects in bilateral SPC, right Putamen (Fig. 5a) as well as the right supplementary motor area (SMA), right parietal operculum (PO) (secondary somatosensory cortex) (Fig. 5c) and bilateral SPC (Fig. 5d). Interaction effects in the right SMA were driven by the LRN group (see Table 4) and therefore identified as sequence-specific. Of note, all clusters in the SPC are overlapping across parameters (DC & EC).

a)

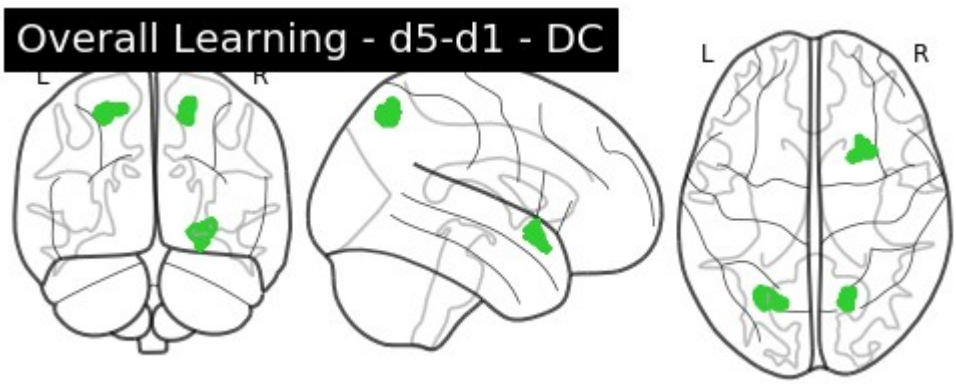

b)

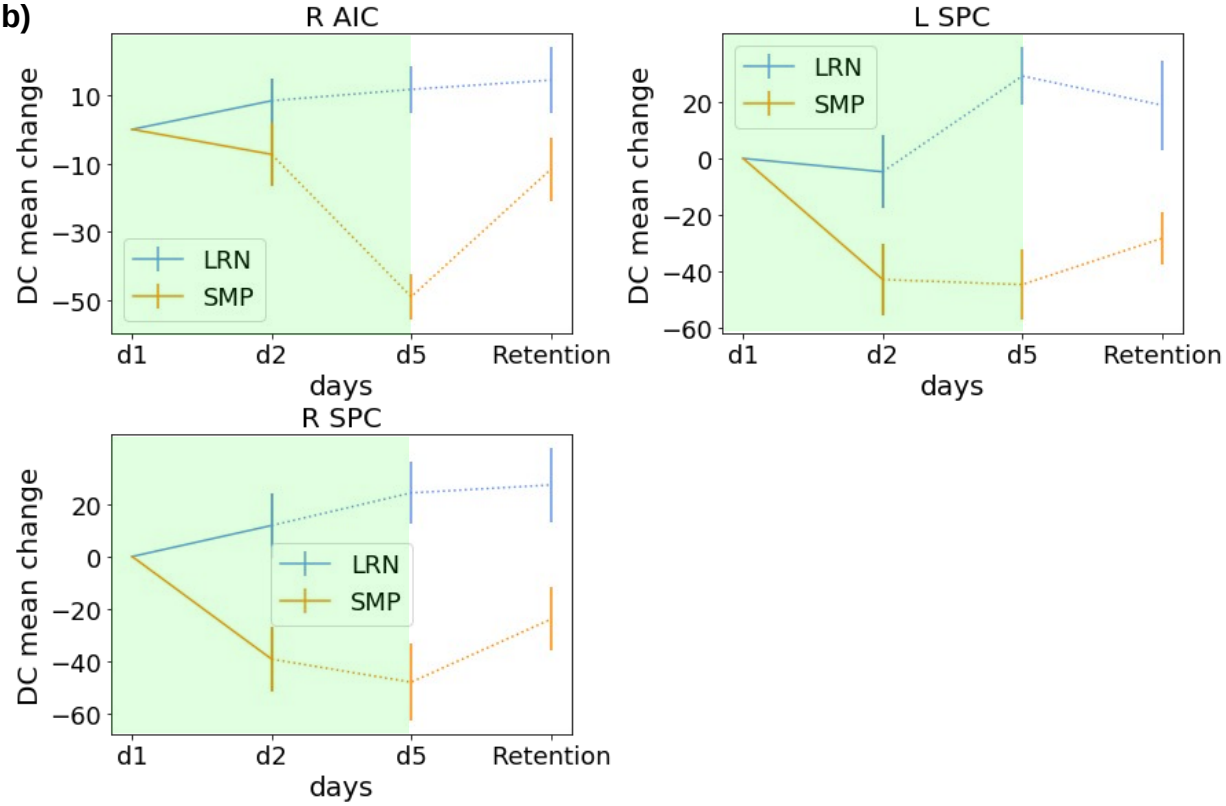
R AIC
L SPC
R SPC
DC mean change
days
d1
d2
d5
Retention
LRN
SMP
10
−10
−30
−50
20
0
−20
−40
−60

c)

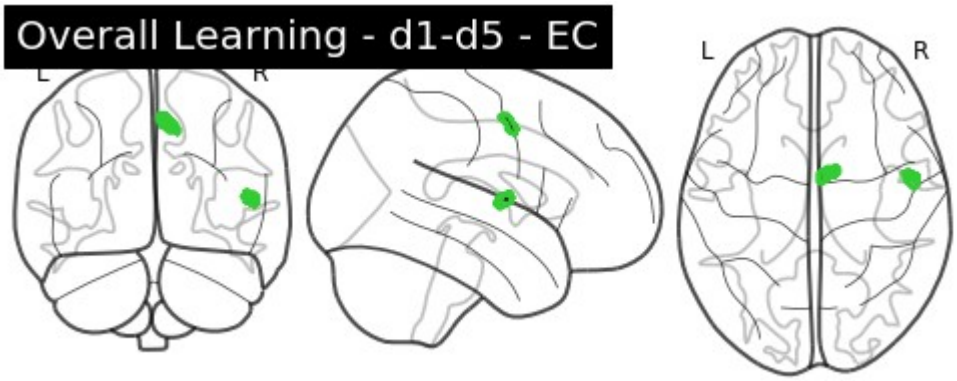
Overall Learning - d1-d5 - EC
L
R

d)

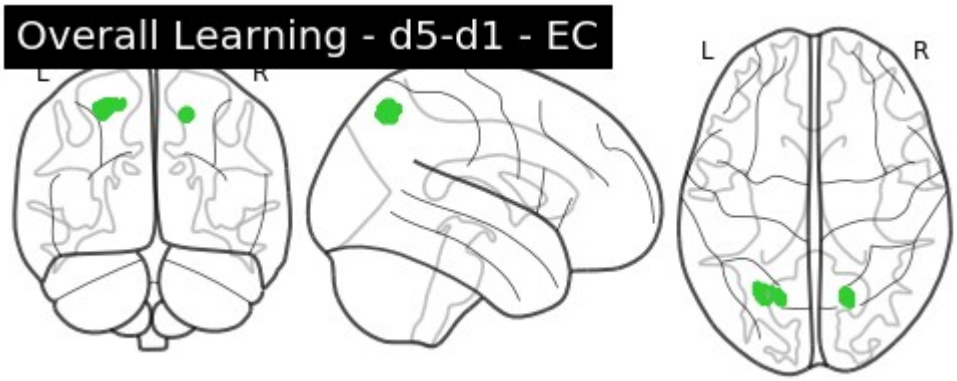
Overall Learning - d5-d1 - EC
L
R

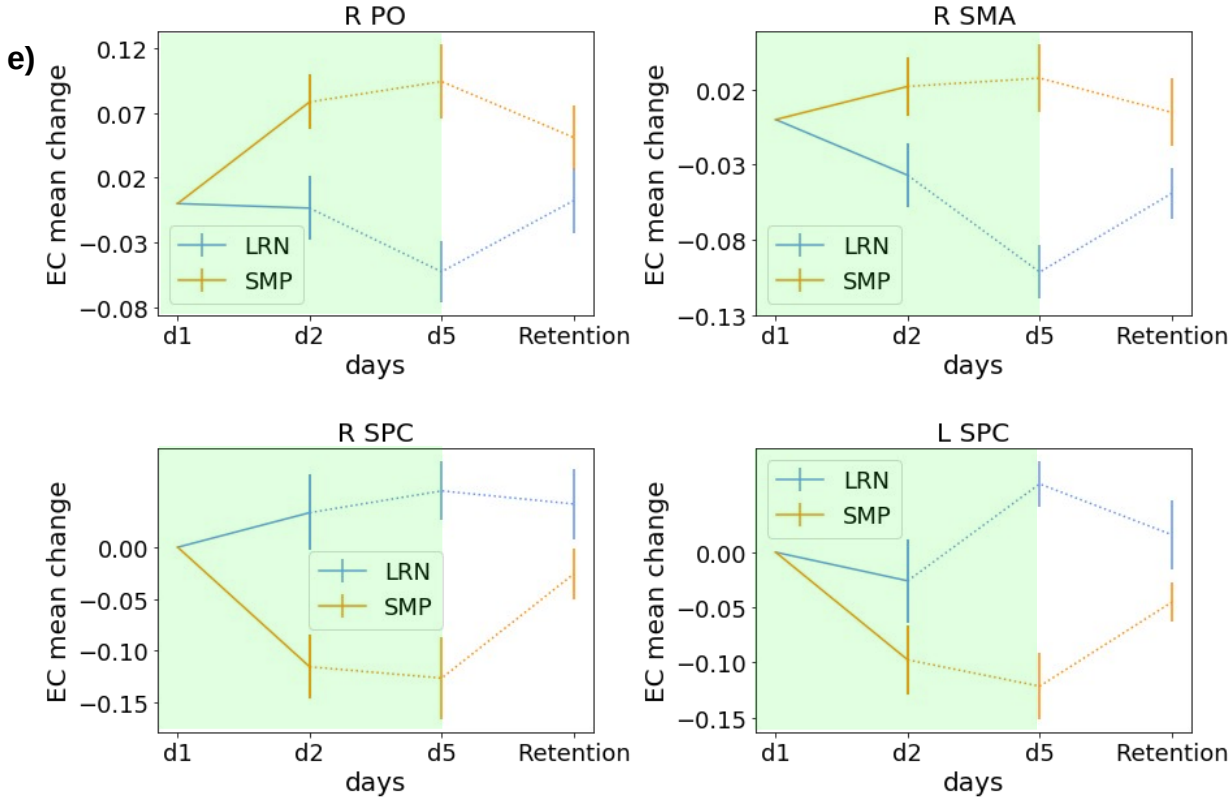

Fig. 5 Group interaction: Overall learning. a) Glass brain DC. d5-d1 interaction effects in the R AIC and bilateral SPC. b) shows the DC change value trajectory over the entire training period for the significant clusters in R AIC and bilateral SPC displayed for LRN and SMP with the period which had the significant interaction (d1/d5) highlighted in green. c) Glass brain EC. d1-d5 interaction effects in the R PO and R SMA (seq-spec.). d) shows the EC change value trajectory over the entire training period for the significant cluster in R AIC displayed for LRN and SMP with the period which had the significant interaction (d2/d5) highlighted in green

Interaction effects - Retention

To identify potential degree centrality changes between the last time point of training and the retention probe, we compared d5 and d17 between the two groups. We identified a significant interaction effect in the left SMA in DC (Fig. 6a) and right Putamen in EC (Fig. 6c). Neither of these effects were predominantly driven by LRN.

a)

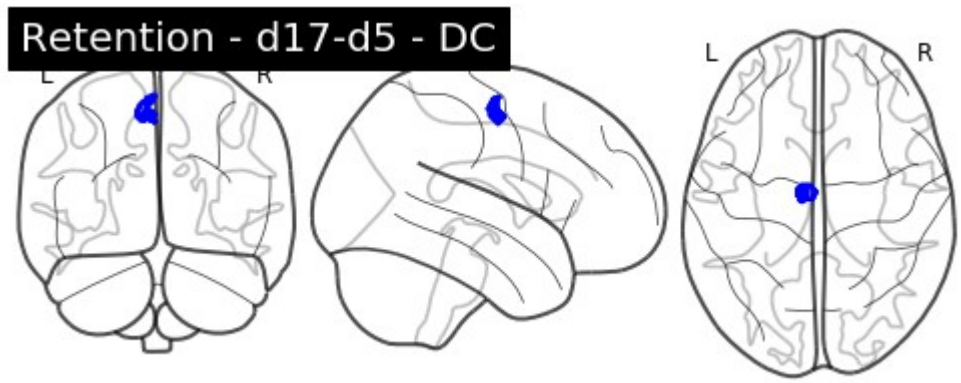
Retention - d17-d5 - DC
L
R

b)

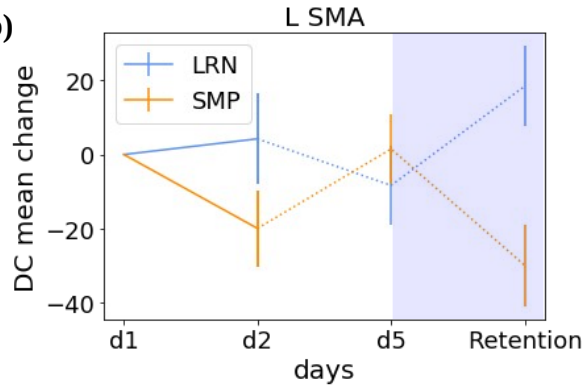
L SMA
LRN
SMP
DC mean change
20
0
−20
−40
d1
d2
d5
Retention
days

c)

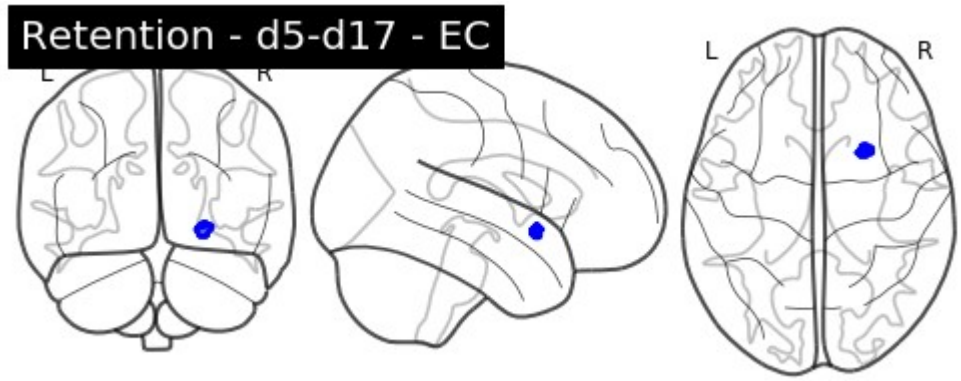
Retention - d5-d17 - EC
L
R

d)

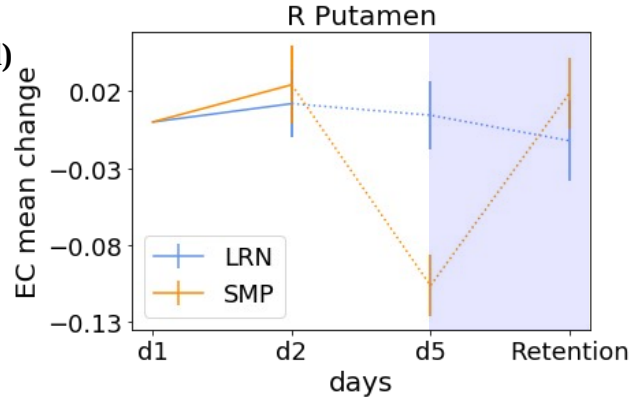
R Putamen
EC mean change
0.02
−0.03
−0.08
−0.13
LRN
SMP
d1
d2
d5
Retention
days

Fig. 6 Group interaction: Retention. a) Glass brain DC. d5-d17 interaction effects in the L SMA. b) shows the DC change value trajectory over the entire training period for the significant clusters in L SMA displayed for LRN and SMP with the period which had the significant interaction (d5/d17) highlighted in blue. c) Glass brain EC. d17-d5 interaction effects in the R Putamen d) shows the EC change value trajectory over the entire training period for the significant cluster in R AIC displayed for LRN and SMP with the period which had the significant interaction (d5/d17) highlighted in blue

Precise locations as well as MNI coordinates of peak voxels and significance thresholds of the significant clusters are listed in Tables 1 and 2.

Table 1: Flexible Factorial Analysis interaction effect results, DC

contrast	pval FDR	K	peak T-value	MNI Coordinates	Anatomical location
d2-d1	0.01	106	4.47	12,-5,-11	R GPi
d2-d1	0.029	88	4.09	-31,-19,56	L M1
d2-d1	0	434	4.06	41, -73, 25	R SOG
d2-d1	0	824	4.01	23,-73,47	R SPC
d5-d2	0	264	4.16	31,12,-10	R AIC
d5-d17	0.013	141	4.24	-8,-11,54	L SMA
d5-d1	0	292	4.84	25,11,-11	R AIC
d5-d1	0	289	4.3	-26,-67,54	L SPC
d5-d1	0.012	264	3.83	18,-65,52	R SPC

Table 2: Flexible Factorial Analysis interaction effect results, EC

Contrast	pval FDR	K	peak T-value	MNI Coordinates	Anatomical location
d1-d2	0.001	144	4.21	35,22, -14	R AIC

d2-d1	0.003	431	3.88	24, -76, 47	R SPC
d5-d2	0	391	4.5	30, 18, -14	R AIC
d17-d5	0.025	27	4.25	24,10,-10	R Putamen
d1-d5	0	131	4.03	6,-4,52	R SMA
d1-d5	0.002	92	3.8	52,-2,7	R PO
d5-d1	0.008	244	4.47	-26,-66,55	L SPC
d5-d1	0.008	88	3.81	17,-65,52	R SPC

Table 3: Summary statistics for regions exhibiting significant time-by-group interactions. Regions where LRN exhibited greater change than SMP are highlighted in grey.

DC		**LRN**			**SMP**		
		MEAN	**SEM**	**95% CI**	**MEAN**	**SEM**	**95% CI**
Fast Learning (d1 vs d2)	R GPi	34.66	8.40	[17.09, 52.24]	-23.23	8.31	[-40.63, -5.84]
	L M1	20.84	13.88	[-8.22, 49.90]	-34.58	7.73	[-50.76, -18.40]

	R SOG	10.9	12.12	[-14.47, 36.26]	-50.46	11.47	[-74.47, -26.45]
	R SPC	23.98	11.55	[-0.19, 48.16]	-46.18	12.76	[-72.90, -19.47]
Slow Learning (d2 vs d5)							
	R AIC	7.66	8.75	[-10.67, 25.98]	-46.40	7.85	[-62.83, -29.97]
Retention (d5 vs d17)							
	L SMA	26.80	9.58	[6.74, 46.86]	-31.42	8.90	[-50.05, -12.79]
Overall Learning (d1 vs d5)							
	R AIC	11.70	7.03	[-3.03, 26.42]	-49.00	6.80	[-63.24, -34.77]
	L SPC	29.10	10.41	[7.29, 50.90)	-44.56	12.61	[-70.96, -18.16]
	R SPC	24.31	12.25	[-1.32, 49.94]	-47.99	14.97	[-79.33, -16.64]

EC		**LRN**			**SMP**		
		MEAN	**SEM**	**95% CI**	**MEAN**	**SEM**	**95% CI**
Fast Learning (d1 vs d2)	R AIC	-0.05	0.03	[-0.10, 0.01]	0.10	0.03	[0.04, 0.16]
	R SPC	0.06	0.03	[-0.01, 0.12]	-0.12	0.03	[-0.19, -0.04]
Slow Learning (d2 vs d5)	R AIC	0.02	0.03	[-0.04, 0.08]	-0.13	0.02	[-0.17, -0.10]

Retention (d5 vs d17)	R Putamen	-0.02	0.02	[-0.06, 0.03]	0.12	0.03	[0.06, 0.19]
Overall Learning (d1 vs d5)	R SMA	-0.10	0.02	[-0.14, -0.06]	0.03	0.02	[-0.02, 0.08]
	R PO	-0.05	0.02	[-0.10, -0.00]	0.09	0.03	[0.03, 0.16]
	L SPC	0.06	0.02	[0.02, 0.11]	-0.12	0.03	[-0.19, -0.06]
	R SPC	0.05	0.03	[-0.01, 0.12]	-0.13	0.04	[-0.21, -0.04]

Correlational Analyses between Sequence-Specific Clusters

a)

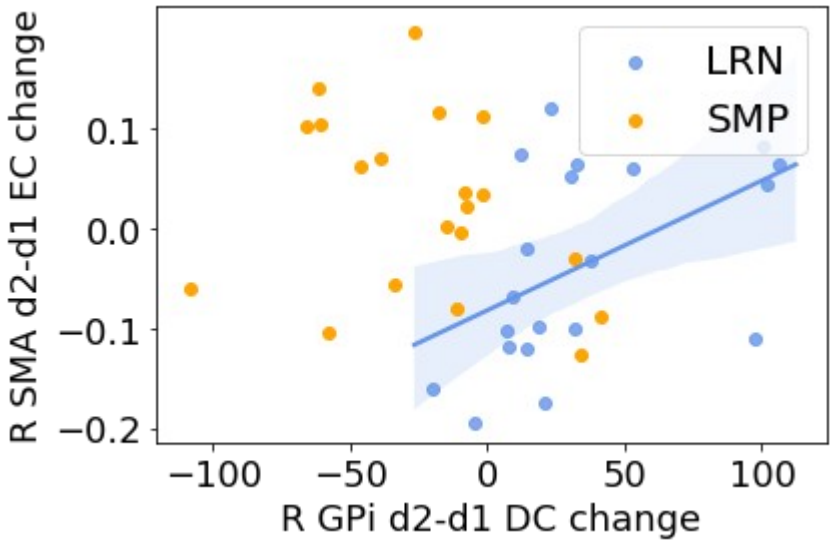

b)

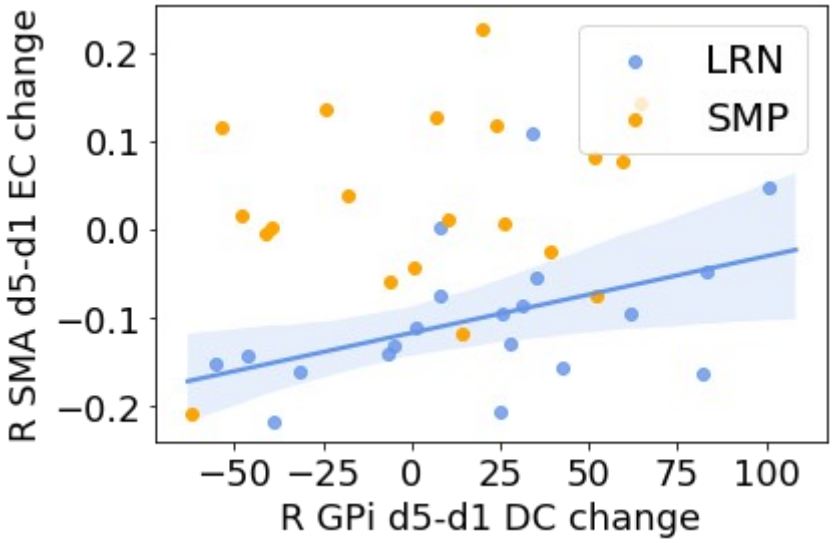

Fig. 7. Correlations between sequence-specific clusters in LRN: a) shows the correlation between DC change values in the right GPi and EC change values in the right SMA for LRN (r = -0.49, p=0.03) (blue) and for SMP (p=0.22) (orange) during fast learning (d2-d1) . **b)** shows the correlation of DC change values in the right GPi with EC change values in the right SMA for LRN (r = -0.46,l.

To investigate a potential relationship between the sequence-specific clusters in the GPi and SMA, we conducted pearson correlation analyses between the mean change scores within our regions of interest (ROIs). We first wanted to know whether the change in GPi during fast learning was related to the change in SMA during the overall learning period, as these were the timescales in which each cluster showed a significant change in the interaction analyses. This was not significant for LRN (p=0.27) nor for SMP (p=0.72). We then wanted to understand whether congruent changes in our ROIs were related and whether there was a more timing-specific relationship during fast or overall learning. We found that the change (d2-d1) of DC in GPi was significantly positively correlated with the change (d2-d1) in EC in

the right SMA for LRN (r = 0.49, p=0.03; Fig. 7) but not for SMP (p=0.22). Subsequently, during overall learning (GPi d5-d1, SMA d5-d1) we also found this correlation to be significant for LRN (r=0.46, p=0.04) and not for SMP (p=0.26).

DISCUSSION

We investigated between-group interaction effects in functional connectivity changes over the course of one week of training on a continuous motor sequence task with rsfMRI. Our study encompasses fast learning, slow learning, overall learning, and retention. Crucially, we compared a group that learned a complex sequence with a control group that performed a matched motor task to distinguish changes due to sequence-specific learning and provide additional context for changes in resting state functional connectivity after MSL throughout the learning stages.

Interaction analyses revealed a set of regions mostly within the motor network that exhibited differential change between the two groups, providing evidence that these regions play a role in functional plasticity after MSL. Our criterion for assigning sequence-specific function to a region was dependent on that region exhibiting greater centrality change in the LRN group. As a result, we found sequence-specific functional changes in two brain regions: the GPi during fast learning and SMA during overall learning. Most of the other regions identified in the interactional analyses, including well known motor learning related areas such as the SPC and M1, also showed opposing centrality changes in both groups but were not being driven by LRN, suggesting differential involvement of these regions when learning a complex motor sequence versus a simpler motor execution.

Sequence-specificity

Sequence-specific learning effects were identified during fast learning in the sensorimotor territory of the GPi, and during the overall learning period in the SMA. We found no

evidence for sequence-specific effects during the slow learning or retention phases. Predominant roles of GPi and SMA in sequence-specificity during offline learning align well with the literature on sequence-specificity from task-based online assessments of MSL (Alexander & Crutcher, 1990, Boecker et al., 2008, Elsinger et al., 2006, Gaymard et al., 1990, Gerloff et al., 1997, Herrojo Ruiz et al., 2014, Hikosaka et al., 1999, Jenkins et al., 1994, Lee & Quessy, 2003, Lehéricy et al., 2005, Mushiake et al., 1991, Mushiake & Strick, 1995, Shima & Tanji, 2000, Tanaka et al., 2010, Ugurbil & Doyon, 2005).

The GPi is one of the main inhibitory output regions of the basal ganglia (Turner & Desmurget, 2010) and plays a major role in regulating voluntary movements (Turner & Anderson, 2005, Gillies et al., 2017). Previous research has shown that this region is involved in online sequence learning with task-based fMRI (Herrojo Ruiz et al., 2014, Lehéricy et al., 2005, Mushiake & Strick, 1995), and has been causally linked to enhanced MSL in Parkinson's patients (Fukuda et al., 2002). The globus pallidus was also identified as one of the few key regions exhibiting sequence-specific change following learning in a recent meta-analysis of online MSL (Janacsek et al., 2020). The increase in DC in the GPi during fast learning indicates that it had more direct connections on d2 than it did on d1. Consequently, it is interesting to note that GPi is directly connected to the SMA, which is one of its main output regions (Akkal et al., 2007). We found a sequence-specific decrease in EC during overall learning (between d1 and d5) in the SMA. Previous research has also shown that the SMA is relevant for sequence-specific MSL during online learning in humans and experiments in nonhuman primates (Alexander & Crutcher, 1990, Dayan and Cohen, 2011, Elsinger et al., 2006, Hikosaka et al., 1999, Jenkins et al., 1994, Krakauer, 2019, Lee & Quessy, 2003, Mushiake et al., 1991), which have established that it is activated during the planning period prior to sequence execution (Tanji & Shima, 1994). Our results provide

support for the role of the SMA in processing sequential information and illustrate how this region is involved in sequence-specific plasticity offline as a result of MSL. We found that EC in the SMA gradually decreased over the entire learning period, suggesting an ongoing relevance to the learning process. While it would be intuitive to interpret a decrease in connectivity as indicating decreased involvement of that area, it is important to keep in mind that EC is a network measure that reflects less connectedness to other highly connected nodes, rather than less activation of the region per se.

Since it is known that SMA connects to GPi structurally (Akkal et al., 2007), which showed an increased number of connections between the first two days of learning, it is reasonable to hypothesize that connectivity changes in both regions may be dependent on one another. Therefore, we investigated the relationship of functional changes between both sequence-specific clusters. We found that, in the LRN group, the change in DC in GPi was significantly positively correlated with the change in EC in SMA during early learning (d1/d2) and overall learning (d1/d5) (Figure 7). We were unable to detect similar significant correlations in the SMP group, indicating that the effect is likely driven by sequence-specific learning. While these correlation analyses were exploratory in nature, they provide additional evidence that the GPi and SMA interact and are important for offline network-level sequence-specific learning during different stages.

Motor execution

Within our interaction analysis we found clusters, mostly within the motor network, that appeared relevant for both groups as the changes were driven by the SMP group. Interestingly, within our trajectory visualizations, we found that the changes in centrality in these regions showed mostly opposite directionalities. The SPC and M1, key nodes in the motor learning network (Dayan & Cohen, 2011, Doyon et al., 2018, Krakauer et al., 2019,

Penhune & Steele, 2012), showed centrality increases in LRN. The hand area of M1 is known to be relevant for finger movements and early motor consolidation (Dechent & Frahm, 2003, Hluštík et al., 2001, Karni et al., 1995, Muellbacher et al., 2002, Yousry et al., 1997, Yokoi et al., 2018), while the SPC is involved in learning the association of visual stimuli and motor actions / visuomotor control (Hardwick et al., 2012, Mutha et al., 2011, Müller et al., 2002), and has been found to be relevant for early and later learning stages (Ma et al., 2011). We observed a steady increase in functional connectivity in both regions from d1 through d5. Considering that the d1/d5 comparison reflects the overall learning process of the LRN group, we propose that the SPC exhibits a slow increase in connectivity over the course of the entire learning period. Interestingly, we found overlapping clusters in SPC across centrality parameters, suggesting that, as the task is learned, functional connections in SPC not only increase in number but also gain relevance within the entire network on a whole brain level. These connectivity increases could reflect a continuous learning process that may serve to integrate the presented visual sequence with the required sequential motor response. It is thus reasonable to conclude that the SPC and M1 are relevant for both LRN and SMP, as the tasks performed by both groups require finger movement and the coordination of visual and motor information. However, they are likely to be less relevant for complex sequence - and sequence-specific learning per se (Berlot et al., 2020).

Limitations

It is difficult to determine the driving factor of connectivity changes in the control group. However, we speculate that these different directionalities of change could be due to task complexity (Carey et al., 2005, Witt et al., 2008). It is possible that SMP, being a rather simple task, would cause centrality changes to occur faster, so that we are looking at a change reflecting a well-learned or overlearned task (motor execution). In contrast, centrality

changes in LRN would rather reflect changes during the actual learning process of the complex sequence within our experimental group.

Conclusion

The present experiment employed a mixed longitudinal training design with two groups (learning and control) to investigate learning on a continuous motor sequence task. We provide evidence for connectivity changes in a subset of regions in the motor learning network that are specific to the learned sequence rather than motor execution: the sensorimotor territory of the right GPi during fast learning and right SMA during overall learning. We also argue that changes in resting state centrality in other regions of the motor network, including M1 and SPC, could be due to motor execution processes common to both tasks. Finally, we provide evidence for a timing- and sequence-specific mechanism between GPi and SMA that would be important to consider for future studies to fully understand offline changes after sequence-specific MSL.

Acknowledgements

We would like to thank Elisabeth Wladimirov and Domenica Wilfling for their help and involvement in data acquisition and logistics of the multi-modal plasticity initiative (MMPI) dataset. This work was supported by the Max Planck Society, the MaxNetAging Research School (Max Planck Institute for Demographic Research, ATJ), the NWO Vici grant (PI: Birte Forstmann)(PLB), the Heart and Stroke Foundation of Canada (CJS, CJG), the Michal and Renata Hornstein Chair in Cardiovascular Imaging (CJG), the National Science and Engineering Research Council (CJS: RGPIN-2020-06812; CJG: RGPIN 2015-04665) and the Fonds Recherche Québécois Nature et Technologies (CJS).

References:

Abraham, A., Pedregosa, F., Eickenberg, M., Gervais, P., Mueller, A., Kossaifi, J., Gramfort, A., Thirion, B., & Varoquaux, G. (2014). Machine learning for neuroimaging with scikit-learn. *Frontiers in Neuroinformatics*, *8*. https://doi.org/10.3389/fninf.2014.00014

Albert, N. B., Robertson, E. M., & Miall, R. C. (2009). The Resting Human Brain and Motor Learning. *Current Biology*, *19*(12), 1023–1027. https://doi.org/10.1016/j.cub.2009.04.028

Avants, B. B., Tustison, N., & Song, G. (2009). Advanced normalization tools (ANTS). *Insight j*, *2*, 1–35.

Bazin, P.-L., Weiss, M., Dinse, J., Schäfer, A., Trampel, R., & Turner, R. (2014). A computational framework for ultra-high resolution cortical segmentation at 7Tesla. *NeuroImage*, *93*, 201–209. https://doi.org/10.1016/j.neuroimage.2013.03.077

Behzadi, Y., Restom, K., Liau, J., & Liu, T. T. (2007). A Component Based Noise Correction Method (CompCor) for BOLD and Perfusion Based fMRI. *NeuroImage*, *37*(1), 90–101. https://doi.org/10.1016/j.neuroimage.2007.04.042

Bengtsson, S. L., Nagy, Z., Skare, S., Forsman, L., Forssberg, H., & Ullén, F. (2005). Extensive piano practicing has regionally specific effects on white matter development. *Nature Neuroscience*, *8*(9), 1148–1150. https://doi.org/10.1038/nn1516

Berlot, E., Popp, N. J., & Diedrichsen, J. (2020). A critical re-evaluation of fMRI signatures of motor sequence learning. *ELife*, *9*, e55241. https://doi.org/10.7554/eLife.55241

Bullmore, E. T., & Bassett, D. S. (2011). Brain Graphs: Graphical Models of the Human Brain Connectome. *Annual Review of Clinical Psychology*, *7*(1), 113–140. https://doi.org/10.1146/annurev-clinpsy-040510-143934

Carey, J. R., Bhatt, E., & Nagpal, A. (2005). Neuroplasticity Promoted by Task

Complexity. *Exercise and Sport Sciences Reviews*, *33*(1), 24–31.

Coynel, D., Marrelec, G., Perlbarg, V., Pélégrini-Issac, M., Van de Moortele, P.-F., Ugurbil, K., Doyon, J., Benali, H., & Lehéricy, S. (2010). Dynamics of motor-related functional integration during motor sequence learning. *NeuroImage*, *49*(1), 759–766. https://doi.org/10.1016/j.neuroimage.2009.08.048

Cusack, R., Brett, M., & Osswald, K. (2003). An Evaluation of the Use of Magnetic Field Maps to Undistort Echo-Planar Images. *NeuroImage*, *18*(1), 127–142. https://doi.org/10.1006/nimg.2002.1281

Dayan, E., & Cohen, L. G. (2011). Neuroplasticity subserving motor skill learning. *Neuron*, *72*(3), 443–454. https://doi.org/10.1016/j.neuron.2011.10.008

Desmurget, M., & Turner, R. S. (2010). Motor Sequences and the Basal Ganglia: Kinematics, Not Habits. *The Journal of Neuroscience*, *30*(22), 7685–7690. https://doi.org/10.1523/JNEUROSCI.0163-10.2010

Dechent, P., & Frahm, J. (2003). Functional somatotopy of finger representations in human primary motor cortex. *Human Brain Mapping*, *18*(4), 272–283. https://doi.org/10.1002/hbm.10084

Doyon, J, Gabitov, E., Vahdat, S., Lungu, O., & Boutin, A. (2018). Current issues related to motor sequence learning in humans. *Current Opinion in Behavioral Sciences*, *20*, 89–97. https://doi.org/10.1016/j.cobeha.2017.11.012

Doyon, Julien, & Benali, H. (2005). Reorganization and plasticity in the adult brain during learning of motor skills. *Current Opinion in Neurobiology*, *15*(2), 161–167. https://doi.org/10.1016/j.conb.2005.03.004

Doyon, Julien, Penhune, V., & Ungerleider, L. G. (2003). Distinct contribution of the cortico-striatal and cortico-cerebellar systems to motor skill learning. *Neuropsychologia*, *41*(3), 252–262. https://doi.org/10.1016/s0028-3932(02)00158-6

Gerloff, C., Corwell, B., Chen, R., Hallett, M., & Cohen, L. G. (1997). Stimulation over the human supplementary motor area interferes with the organization of future elements in complex motor sequences. *Brain: A Journal of Neurology*, *120 (Pt 9)*, 1587–1602. https://doi.org/10.1093/brain/120.9.1587

Gillies, M. J., Hyam, J. A., Weiss, A. R., Antoniades, C. A., Bogacz, R., Fitzgerald, J. J., Aziz, T. Z., Whittington, M. A., & Green, A. L. (2017). The Cognitive Role of the Globus Pallidus interna; Insights from Disease States. *Experimental Brain Research*, *235*(5), 1455–1465. https://doi.org/10.1007/s00221-017-4905-8

Gorgolewski, K. J., Esteban, O., Burns, C., Ziegler, E., Pinsard, B., Madison, C., Waskom, M., Ellis, D. G., Clark, D., Dayan, M., Manhães-Savio, A., Notter, M. P., Johnson, H., Dewey, B. E., Halchenko, Y. O., Hamalainen, C., Keshavan, A., Clark, D., Huntenburg, J. M., … Ghosh, S. (2016). *Nipype: A flexible, lightweight and extensible neuroimaging data processing framework in Python. 0.12.0-rc1*. Zenodo. https://doi.org/10.5281/zenodo.50186

Gregory, M. D., Agam, Y., Selvadurai, C., Nagy, A., Vangel, M., Tucker, M., Robertson, E. M., Stickgold, R., & Manoach, D. S. (2014). Resting state connectivity immediately following learning correlates with subsequent sleep-dependent enhancement of motor task performance. *NeuroImage*, *102*(0 2), 666–673. https://doi.org/10.1016/j.neuroimage.2014.08.044

Gryga, M., Taubert, M., Dukart, J., Vollmann, H., Conde, V., Sehm, B., Villringer, A., & Ragert, P. (2012). Bidirectional gray matter changes after complex motor skill learning. *Frontiers in Systems Neuroscience*, *6*. https://doi.org/10.3389/fnsys.2012.00037

Hardwick, R. M., Rottschy, C., Miall, R. C., & Eickhoff, S. B. (2013). A quantitative meta-analysis and review of motor learning in the human brain. *Neuroimage*, *67*, 283–297. https://doi.org/10.1016/j.neuroimage.2012.11.020

Hikosaka, O., Nakahara, H., Rand, M. K., Sakai, K., Lu, X., Nakamura, K., Miyachi,

S., & Doya, K. (1999). Parallel neural networks for learning sequential procedures. *Trends in Neurosciences*, *22*(10), 464–471.

Hluštík, P., Solodkin, A., Gullapalli, R. P., Noll, D. C., & Small, S. L. (2001). Somatotopy in Human Primary Motor and Somatosensory Hand Representations Revisited. *Cerebral Cortex*, *11*(4), 312–321. https://doi.org/10.1093/cercor/11.4.312

Janacsek, K., Shattuck, K. F., Tagarelli, K. M., Lum, J. A. G., Turkeltaub, P. E., & Ullman, M. T. (2020). Sequence learning in the human brain: A functional neuroanatomical meta-analysis of serial reaction time studies. *NeuroImage*, 116387. https://doi.org/10.1016/j.neuroimage.2019.116387

Jenkinson, M. (2004), Improving the registration of B0- distorted EPI images using calculated cost function weights. *10th Int. Conference on Functional Mapping of the Human Brain.*

Karim, H. T., Huppert, T. J., Erickson, K. I., Wollam, M. E., Sparto, P. J., Sejdić, E., & VanSwearingen, J. M. (2017). Motor Sequence Learning-Induced Neural Efficiency in Functional Brain Connectivity. *Behavioural Brain Research*, *319*, 87–95. https://doi.org/10.1016/j.bbr.2016.11.021

Karni, A., Meyer, G., Jezzard, P., Adams, M. M., Turner, R., & Ungerleider, L. G. (1995). Functional MRI evidence for adult motor cortex plasticity during motor skill learning. *Nature*, *377*(6545), 155–158. https://doi.org/10.1038/377155a0

Krakauer, J. W., Hadjiosif, A. M., Xu, J., Wong, A. L., & Haith, A. M. (2019). Motor Learning. *Comprehensive Physiology*, *9*(2), 613–663. https://doi.org/10.1002/cphy.c170043

Lehéricy, S., Benali, H., Van de Moortele, P.-F., Pélégrini-Issac, M., Waechter, T., Ugurbil, K., & Doyon, J. (2005). Distinct basal ganglia territories are engaged in early and advanced motor sequence learning. *Proceedings of the National Academy of Sciences of the United States of America*, *102*(35), 12566–12571. https://doi.org/10.1073/pnas.0502762102

Lewis, C. M., Baldassarre, A., Committeri, G., Romani, G. L., & Corbetta, M. (2009). Learning sculpts the spontaneous activity of the resting human brain. *Proceedings of the National Academy of Sciences*, *106*(41), 17558–17563. https://doi.org/10.1073/pnas.0902455106

Lohmann, G., Margulies, D. S., Horstmann, A., Pleger, B., Lepsien, J., Goldhahn, D., Schloegl, H., Stumvoll, M., Villringer, A., & Turner, R. (2010). Eigenvector Centrality Mapping for Analyzing Connectivity Patterns in fMRI Data of the Human Brain. *PLOS ONE*, *5*(4), e10232. https://doi.org/10.1371/journal.pone.0010232

Lohse, K.R., Wadden, K., Boyd, L.A., & Hodges, N.J. (2014). Motor skill acquisition across short and long time scales: A meta-analysis of neuroimaging data. *Neuropsychologia*, *59*, 130–141. https://doi.org/10.1016/j.neuropsychologia.2014.05.001

Ma, L., Narayana, S., Robin, D. A., Fox, P. T., & Xiong, J. (2011). Changes Occur in Resting State Network of Motor System during 4 Weeks of Motor Skill Learning. *NeuroImage*, *58*(1), 226–233. https://doi.org/10.1016/j.neuroimage.2011.06.014

Mary, A., Wens, V., Op de Beeck, M., Leproult, R., De Tiège, X., & Peigneux, P. (2017). Resting-state Functional Connectivity is an Age-dependent Predictor of Motor Learning Abilities. *Cerebral Cortex (New York, N.Y.: 1991)*, *27*(10), 4923–4932. https://doi.org/10.1093/cercor/bhw286

Muellbacher, W., Ziemann, U., Wissel, J., Dang, N., Kofler, M., Facchini, S., Boroojerdi, B., Poewe, W., & Hallett, M. (2002). Early consolidation in human primary motor cortex. *Nature*, *415*(6872), 640–644. https://doi.org/10.1038/nature712

Müller, R.-A., Kleinhans, N., Pierce, K., Kemmotsu, N., & Courchesne, E. (2002). Functional MRI of motor sequence acquisition: Effects of learning stage and performance. *Cognitive Brain Research*, *14*(2), 277–293. https://doi.org/10.1016/S0926-6410(02)00131-3

Mutha, P. K., Sainburg, R. L., & Haaland, K. Y. (2011). Left Parietal Regions Are

Critical for Adaptive Visuomotor Control. *The Journal of Neuroscience*, *31*(19), 6972–6981. https://doi.org/10.1523/JNEUROSCI.6432-10.2011

Penhune, V. B., & Steele, C. J. (2012). Parallel contributions of cerebellar, striatal and M1 mechanisms to motor sequence learning. *Behavioural Brain Research*, *226*(2), 579–591. https://doi.org/10.1016/j.bbr.2011.09.044

Poldrack, R., Mumford, J. & Nichols, T. *Handbook of Functional MRI Data Analysis* (Cambridge University Press, 2011).

Roche, A. (2011). A Four-Dimensional Registration Algorithm With Application to Joint Correction of Motion and Slice Timing in fMRI. *IEEE Transactions on Medical Imaging*, *30*(8), 1546–1554. https://doi.org/10.1109/TMI.2011.2131152

Rosenbaum, D. A., Kenny, S. B., & Derr, M. A. (1983). Hierarchical control of rapid movement sequences. *Journal of Experimental Psychology. Human Perception and Performance*, *9*(1), 86–102.

Sami, S., & Miall, R. C. (2013). Graph network analysis of immediate motor-learning induced changes in resting state BOLD. *Frontiers in Human Neuroscience*, *7*. https://doi.org/10.3389/fnhum.2013.00166

Sami, Saber, Robertson, E. M., & Miall, R. C. (2014). The Time Course of Task-Specific Memory Consolidation Effects in Resting State Networks. *Journal of Neuroscience*, *34*(11), 3982–3992. https://doi.org/10.1523/JNEUROSCI.4341-13.2014

Scholz, J., Klein, M. C., Behrens, T. E. J., & Johansen-Berg, H. (2009). Training induces changes in white-matter architecture. *Nature Neuroscience*, *12*(11), 1370–1371. https://doi.org/10.1038/nn.2412

Seidler, R. D., Purushotham, A., Kim, S.-G., Uğurbil, K., Willingham, D., & Ashe, J. (2002). Cerebellum Activation Associated with Performance Change but Not Motor Learning. *Science*, *296*(5575), 2043–2046. https://doi.org/10.1126/science.1068524

Steel, A., Thomas, C., Trefler, A., Chen, G., & Baker, C. I. (2019). Finding the baby in the bath water – evidence for task-specific changes in resting state functional connectivity evoked by training. *NeuroImage*, *188*, 524–538. https://doi.org/10.1016/j.neuroimage.2018.12.038

Steele, C. J., & Penhune, V. B. (2010). Specific Increases within Global Decreases: A Functional Magnetic Resonance Imaging Investigation of Five Days of Motor Sequence Learning. *Journal of Neuroscience*, *30*(24), 8332–8341. https://doi.org/10.1523/JNEUROSCI.5569-09.2010

Tanaka, S., Honda, M., Hanakawa, T., & Cohen, L. G. (2010). Differential Contribution of the Supplementary Motor Area to Stabilization of a Procedural Motor Skill Acquired through Different Practice Schedules. *Cerebral Cortex (New York, NY)*, *20*(9), 2114–2121. https://doi.org/10.1093/cercor/bhp276

Taubert, M., Villringer, A., & Ragert, P. (2012). Learning-Related Gray and White Matter Changes in Humans: An Update. *The Neuroscientist*, *18*(4), 320–325. https://doi.org/10.1177/1073858411419048

Thomas, C., & Baker, C. I. (2013). Teaching an adult brain new tricks: A critical review of evidence for training-dependent structural plasticity in humans. *NeuroImage*, *73*, 225–236. https://doi.org/10.1016/j.neuroimage.2012.03.069

Turner, R. S., & Anderson, M. E. (2005). Context-Dependent Modulation of Movement-Related Discharge in the Primate Globus Pallidus. *The Journal of Neuroscience*, *25*(11), 2965–2976. https://doi.org/10.1523/JNEUROSCI.4036-04.2005

Turner, R. S., & Desmurget, M. (2010). Basal Ganglia Contributions to Motor Control: A Vigorous Tutor. *Current Opinion in Neurobiology*, *20*(6), 704–716. https://doi.org/10.1016/j.conb.2010.08.022

Vahdat, S., Darainy, M., Milner, T. E., & Ostry, D. J. (2011). Functionally specific

changes in resting-state sensorimotor networks following motor learning. *The Journal of Neuroscience*, *31*(47), 16907–16915. https://doi.org/10.1523/JNEUROSCI.2737-11.2011

Virtanen, P., Gommers, R., Oliphant, T. E., Haberland, M., Reddy, T., Cournapeau, D., Burovski, E., Peterson, P., Weckesser, W., Bright, J., van der Walt, S. J., Brett, M., Wilson, J., Millman, K. J., Mayorov, N., Nelson, A. R. J., Jones, E., Kern, R., Larson, E., … van Mulbregt, P. (2020). SciPy 1.0: Fundamental algorithms for scientific computing in Python. *Nature Methods*, *17*(3), 261–272. https://doi.org/10.1038/s41592-019-0686-2

Wang, J., Zuo, X., & He, Y. (2010). Graph-based network analysis of resting-state functional MRI. *Frontiers in Systems Neuroscience*, *4*. https://doi.org/10.3389/fnsys.2010.00016

Wiestler, T., & Diedrichsen, J. (2013). Skill learning strengthens cortical representations of motor sequences. *ELife*, *2*, e00801. https://doi.org/10.7554/eLife.00801

Wink, A. M., de Munck, J. C., van der Werf, Y. D., van den Heuvel, O. A., & Barkhof, F. (2012). Fast Eigenvector Centrality Mapping of Voxel-Wise Connectivity in Functional Magnetic Resonance Imaging: Implementation, Validation, and Interpretation. *Brain Connectivity*, *2*(5), 265–274. https://doi.org/10.1089/brain.2012.0087

Witt, S. T., Laird, A. R., & Meyerand, M. E. (2008). Functional neuroimaging correlates of finger-tapping task variations: An ALE meta-analysis. *NeuroImage*, *42*(1), 343–356. https://doi.org/10.1016/j.neuroimage.2008.04.025

Woo, C.-W., Krishnan, A., & Wager, T. D. (2014). Cluster-extent based thresholding in fMRI analyses: Pitfalls and recommendations. *NeuroImage*, *91*, 412–419. https://doi.org/10.1016/j.neuroimage.2013.12.058

Wymbs, N. F., & Grafton, S. T. (2015). The Human Motor System Supports Sequence-Specific Representations over Multiple Training-Dependent Timescales. *Cerebral Cortex (New York, N.Y.: 1991)*, *25*(11), 4213–4225. https://doi.org/10.1093/cercor/bhu144

Xiong, J., Ma, L., Wang, B., Narayana, S., Duff, E. P., Egan, G. F., & Fox, P. T. (2009). Long-term motor training induced changes in regional cerebral blood flow in both task and resting states. *NeuroImage*, *45*(1), 75–82. https://doi.org/10.1016/j.neuroimage.2008.11.016

Yokoi, A., Arbuckle, S. A., & Diedrichsen, J. (2018). The Role of Human Primary Motor Cortex in the Production of Skilled Finger Sequences. *The Journal of Neuroscience*, *38*(6), 1430–1442. https://doi.org/10.1523/JNEUROSCI.2798-17.2017

Yokoi, A., & Diedrichsen, J. (2019). Neural Organization of Hierarchical Motor Sequence Representations in the Human Neocortex. *Neuron*. https://doi.org/10.1016/j.neuron.2019.06.017

Yousry, T. A., Schmid, U. D., Alkadhi, H., Schmidt, D., Peraud, A., Buettner, A., & Winkler, P. (1997). Localization of the motor hand area to a knob on the precentral gyrus. A new landmark. *Brain*, *120*(1), 141–157. https://doi.org/10.1093/brain/120.1.141

Zuo, X.-N., Ehmke, R., Mennes, M., Imperati, D., Castellanos, F. X., Sporns, O., & Milham, M. P. (2012). Network centrality in the human functional connectome. *Cerebral Cortex (New York, N.Y.: 1991)*, *22*(8), 1862–1875. https://doi.org/10.1093/cercor/bhr269